NEOPLASIA
www.neoplasia.com

Volume 15 Number 7 July 2013 pp. 761–772 761

Cross Modulation between the Androgen Receptor Axis and Protocadherin-PC in Mediating Neuroendocrine Transdifferentiation and Therapeutic Resistance of Prostate Cancer[1,2]

Stéphane Terry[*,†,‡], Pascale Maillé[§], Habiba Baaddi[*,†], Laurence Kheuang[*,†], Pascale Soyeux[*,†], Nathalie Nicolaiew[*,†], Jocelyn Ceraline[¶], Virginie Firlej[*,†], Himisha Beltran[#], Yves Allory[*,†,§,3], Alexandre de la Taille[*,†,,3] and Francis Vacherot[*,†,3]**

*INSERM, Unité 955, Créteil, France; [†]Université Paris-Est Créteil, Créteil, France; [‡]CNRS UMR3244, Centre de Recherche, Institut Curie, Paris, France; [§]Département de Pathologie, Plateforme de Ressources Biologiques, Hôpital H. Mondor–A. Chenevier, AP-HP, Créteil, France; [¶]Faculté de Médecine/Signalisation et Cancer de la Prostate/EA4438, Université Strasbourg, Strasbourg, France; [#]Department of Medicine, Weill Cornell Medical College, New York, NY; **Service d'urologie, Hôpital H. Mondor–A. Chenevier, AP-HP, Créteil, France

Abstract

Castration-resistant prostate cancers (CRPCs) that relapse after androgen deprivation therapies (ADTs) are responsible for the majority of mortalities from prostate cancer (PCa). While mechanisms enabling recurrent activity of androgen receptor (AR) are certainly involved in the development of CRPC, there may be factors that contribute to the process including acquired neuroendocrine (NE) cell–like behaviors working through alternate (non-AR) cell signaling systems or AR-dependent mechanisms. In this study, we explore the potential relationship between the AR axis and a novel putative marker of NE differentiation, the human male protocadherin-PC (PCDH-PC), *in vitro* and in human situations. We found evidence for an NE transdifferentiation process and PCDH-PC expression as an early-onset adaptive mechanism following ADT and elucidate AR as a key regulator of PCDH-PC expression. PCDH-PC overexpression, in turn, attenuates the ligand-dependent activity of the AR, enabling certain prostate tumor clones to assume a more NE phenotype and promoting their survival under diverse stress conditions. Acquisition of an NE phenotype by PCa cells positively correlated with resistance to cytotoxic agents including docetaxel, a taxane chemotherapy approved for the treatment of patients with metastatic CRPC. Furthermore, knockdown of PCDH-PC in cells that have undergone an NE transdifferentiation partially sensitized cells to docetaxel. Together, these results reveal a reciprocal regulation between the AR axis and PCDH-PC signals, observed both *in vitro* and *in vivo*, with potential implications in coordinating NE transdifferentiation processes and progression of PCa toward hormonal and chemoresistance.

Neoplasia (2013) 15, 761–772

Abbreviations: ADT, androgen deprivation therapy; AR, androgen receptor; CRPC, castration-resistant prostate cancer; DHT, dihydrotestosterone; NE, neuroendocrine; PCDH-PC, protocadherin-PC

Address all correspondence to: Dr Stéphane Terry, INSERM, Unité 955, Equipe 7, 8 rue du Général Sarrail, 94000 Créteil, France. E-mail: stephane.terry@gmail.com

[1]This work was supported by INSERM and Université Paris-Est Créteil, through grants from the Association pour la Recherche sur les Tumeurs de la Prostate (to S.T.), by the Fondation ARC pour la Recherche sur le Cancer (to F.V.), and by the Association Française d'Urologie (to A.D.L.T.). This work has been supported by institutional and charity grants only and there are no financial or other interest in the publication of this paper that might be considered a conflict of interest.

[2]This article refers to supplementary materials, which are designated by Tables W1 to W3 and Figures W1 to W6 and are available online at www.neoplasia.com.

[3]Equal contribution.

Received 8 December 2012; Revised 14 April 2013; Accepted 15 April 2013

DOI 10.1593/neo.122070

Introduction

Prostate cancer (PCa) is the most commonly diagnosed malignancy among men in Western nations [1]. It is well recognized that androgens working through the androgen receptor (AR), play a key role in PCa disease initiation and progression [2] and are known to stimulate the PCa cell growth and diminish their rate of apoptosis. This is the basis for the use of androgen deprivation therapy (ADT) in the form of medical or surgical castration as standard frontline therapy for patient with advanced disease [3]. Despite the fact that ADT has been proven to extend life span in accordance with its effect of limiting the growth of "androgen-sensitive" PCa cells and inducing cell death of "androgen-dependent" PCa cells, one important aspect of PCa is that the majority of cases eventually develop resistance to ADT and castration-resistant prostate cancer (CRPC) emerges. Although there are a number of approved and promising therapies for metastatic CRPC, including taxane chemotherapies (i.e., docetaxel, cabazitaxel) and potent AR-targeted agents (i.e., abiraterone, MDV3100) [4], all patients develop resistance, and as such, metastatic CRPC accounts for most PCa-related deaths.

A key mechanism involved in progression of PCa from a hormone-sensitive to castration-resistant state includes acquisition of molecular alterations of the androgen/AR axis, such that PCa cells retain active AR even in the setting of castrate levels of circulating testosterone [5]. However, an alternative mechanism that dominates in some cases of CRPC involves transformation toward an androgen-independent state, in which certain PCa cells offset their sensitivity to androgens by altering their apoptotic pathways such that active androgen/AR signaling is no longer mandatory for their survival. These androgen-independent cell populations may either arise from progenitor or neuroendocrine (NE)–like cells in the primary prostate tumor or from prostate adenocarcinoma cells that transdifferentiate to NE-like cells. It has been more than a decade since the concept first emerged from *in vitro* studies suggesting the latter, that under certain circumstances, including hormonal manipulation, PCa cells have the potential to transdifferentiate to acquire NE characteristics [6–10]. Despite evidence of upregulated NE differentiation in patients receiving ADT [11,12], the origin of NE cells in the prostate remains uncertain. Moreover, the relative lack of knowledge regarding the chain of events and the mechanistic paradigm underlying the transdifferentiation process supports the need for further investigations.

We previously reported that overexpression of *protocadherin-PC* (*PCDH-PC*, also referred to as *PCDH11Y*), a gene primarily identified for its antiapoptotic properties that encodes from the Y-chromosome at Yp11.2 [13,14], can drive NE transdifferentiation in LNCaP [15], a cell line originally established from a lymph node metastatic lesion of human PCa characterized by its androgen-dependent growth [16]. Here, by exploring the potential relationship between the androgen/AR axis and PCDH-PC, we investigated the possibility that PCa progression toward androgen independence is indeed characterized by a putative subpopulation of cancer cells that undergo an NE transdifferentiation. We also explore the extent to which the emergence of these populations is influenced by current therapies for advanced CRPC.

Materials and Methods

Cell Culture and Chemicals

The human PCa cell lines LNCaP and 22Rv1 were obtained from ATCC (Manassas, VA), authenticated at this site, and maintained in recommended medium. For androgen-reduced conditions, cells were cultured in phenol red–free RPMI supplemented with 10% dextran charcoal-stripped FBS (CS-FBS). The LNCaP–PCDH-PC cells were previously described [17]. Steroids and chemotherapeutic agents were obtained from Sigma-Aldrich (St Quentin Fallavier, France). Bicalutamide was obtained from LKT Laboratories (St Paul, MN).

Human Prostate Tissue Samples

The prostate samples have been collected as part of an Institutional Review Board-approved protocol at Henri Mondor Hospital. Specimens consisted of formalin-fixed paraffin-embedded (FFPE) tissues from hormone-naïve PCa (HNPC; n = 222), neoadjuvant hormone therapy–treated PCa (HTPC; n = 32) obtained from radical prostatectomy specimens, and CRPC specimens (n = 60), of which 54 were collected at the time of the transurethral resection of the prostate for obstructive CRPC and 6 isolated from rapid autopsy specimens with metastatic lesions. The study also included a few specimens derived from normal prostates of young donors.

Immunohistochemistry and Immunofluorescence

Paraffin-embedded tissues were sectioned at 5-μm thickness and deparaffinized, and endogenous peroxidase activity was inactivated in a solution containing 3% hydrogen peroxide (H_2O_2) for 10 minutes. Sections were then cleared in running water followed by phosphate-buffered saline. Antigen unmasking was performed by heat retrieval with citrate buffer (pH 6; Dako, Trappes, France). The primary antibodies used are listed in Table W1. Antibodies purified from HB 0337 SSA hybridoma and raised against PCDH-PC are available upon request to Prof. F. Vacherot (vacherot@u-pec.fr). Biotin-labeled antibodies (Jackson ImmunoResearch, New Market, United Kingdom) were used as secondary antibodies. Antigen-antibody reactions were revealed using the streptavidin method with DAB as substrate. All slides were read by a genitourinary pathologist (Y.A.) and the intensity of staining was scored as null (0), weak (1), moderate (2), and strong (3). In this analysis, a case was considered positive only when the score was 2 or more in at least 10% of cancer cells, whereas cases with less than 10% staining or scored below 2 were considered as negative. For dual immunofluorescence staining, samples were processed as above but using, as secondary antibodies, anti-mouse Alexa Fluor 488 (Life Technologies, Grand Island, NY) and biotinylated anti-rabbit antibodies (Jackson ImmunoResearch) with subsequent incubation with Streptavidin-Fluoprobes 647H (Interchim, Montluçon, France). Slides were mounted using Vectashield mounting medium (Vector Laboratories, Burlingame, CA) and inspected by confocal microscopy.

Transient Transfection and Luciferase Reporter Assays

Transient transfection assays and measures of luciferase and β-galactosidase (β-Gal) activities were performed as previously described [15] with minor modifications. The PSA-61-luc plasmid was described previously [18] and used as reporter of AR activity. Briefly, cells (6×10^5 per well) were plated onto 24-well plates and cotransfected the next day using Lipofectamine 2000 (Life Technologies) mixed with up to 400 ng of pcDNA3-PCDH-PC vector or empty pcDNA3 along with 500 ng of a PSA-61-luc and 50 ng of a Lac-Z luciferase plasmid as a transfection control, so that all wells received ~1 μg of DNA. On the next day, cells were treated with dihydrotestosterone (DHT) for 24 hours after which cell lysates were prepared and processed for luciferase activity and β-Gal activity using the Luciferase Reporter Assay and β-Gal Reporter Gene Assay Kits (Roche Diagnostics, Meylan, France), respectively. Measures have been performed using Wallac VICTOR^3 1420 Multilabel Counter (Perkin-Elmer, Courtaboeuf, France).

PCDH-PC Knockdown

All siRNAs were from Thermo Scientific (Waltham, MA). Knockdown of PCDH-PC in 22Rv1 cells was performed using ON-TARGET*plus* *SMART*pool Human PCDH11Y (L-013624); 100 nM ON-TARGET*plus* Non-Targeting Pool (D-001810) or siRNAs against PCDH-PC were transfected in 22Rv1 cells as indicated using Lipofectamine 2000. Knockdown of PCDH-PC in LNCaP–NE-like cells was carried out using Accell *SMART*pool Human PCDH11Y (E-013624). Accell Non-Targeting Pool D-001910 and Accell Green Non-Targeting siRNA were also used. LNCaP–NE-like cells were incubated in Accell siRNA Delivery Media mixed with either 1 μM of Non-Targeting siRNAs or siRNAs against PCDH-PC according to the manufacturer's instructions. On the next day, media were changed and cells were subsequently cultured in the indicated medium.

Cell Growth and Cell Viability

Cell growth was monitored by cell counting and the population doubling time (DT) was estimated (in hours) by using the following formula: $DT = h * \ln(2)/\ln(C2/C1)$, where C1 and C2 are the cell concentrations at the beginning and the end of the chosen period of time. Cell viability was assessed by the tetrazolium bromide (MTT) assay [19] or WST-1 assay (Roche Diagnostics) as described previously [20].

Western Blot Analysis

Protein lysates were prepared and processed as described previously [21].

cDNA Synthesis and Real-Time Polymerase Chain Reaction

RNA was extracted using the TRIzol reagent (Life Technologies), subjected to DNase treatment (DNA-Free Kit; Applied Biosystems, Foster City, CA) according to the manufacturer's instructions. One microgram of total RNA was then reverse transcribed using SuperScript II (Life Technologies). Quantitative polymerase chain reaction (qPCR) was performed using SYBR Green dye on a StepOnePlus Real-Time PCR System (Applied Biosystems). Unless indicated, the amount of each target gene relative to the housekeeping gene *RPLP0* or *HMBS* was determined for each sample using $2^{-\Delta\Delta CT}$ method. Primer sequences are provided in Table W2.

Statistical Analysis

For qualitative data, χ^2 test and Fisher exact test were applied. For *in vitro* studies, comparisons between groups were performed using the Student's *t* test. All statistical tests used a two-tailed $\alpha = 0.05$ level of significance and were performed using GraphPad Prism (GraphPad Software, La Jolla, CA).

Results

Phenotypic Changes in the PCa Cell Line LNCaP upon Androgen Depletion

LNCaP cells are commonly used *in vitro* to model the response to ADT of PCa in patients following hormone manipulation [22]. Thus, we first searched for perturbation in *PCDH-PC* expression and various markers in LNCaP cells maintained in androgen-depleted medium for an extended period. This included known androgen-upregulated gene products *KLK3* (PSA) and *KLK2*, previously described androgen-repressed genes, the neuron-specific enolase (NSE) [6], *neuronal class III β-tubulin* (*TUBB3*) [7], and the hedgehog ligand *SHH* [23], as well as various genes assumed to be critical in PCa progression comprising Bcl-2, Akt, TP53, *MYC*, and AR [5,24]. Western blot (WB) and quantitative reverse transcription–polymerase chain reaction (qRT-PCR) analyses showed that when cells are switched to androgen-deficient medium, NSE and *TUBB3*, two prominent markers of NE differentiation, are induced along with *PCDH-PC*, which shows a peak expression (~125-fold increase) at 2 weeks (Figures 1, *A* and *B*, and W1*A*). *SHH* was also augmented (Figure W1*B*). This period was associated with a decreased of cell growth accompanied by the emergence of neurite-like outgrowths from the cells (Figure 1*C*). We likewise observed a down-regulation of PSA and *KLK2* levels, two AR target genes, during the first weeks of androgen depletion, as expected. We also noted some increase in phosphorylated Akt and a decrease in expression of p53 and *MYC* (Figures 1, *A* and *B*, and W1*A*). Intriguingly, *PCDH-PC* expression was found to be gradually decreased with time in conjunction with reappearance of an epithelial-like morphology and a loss of neurite outgrowth (Figure 1*C*). After 3 months of culturing in androgen-depleted medium, PSA and *KLK2* were again detected, suggestive of AR activity (Figures 1, *A* and *B*, and W1*A*). This was concomitant with the down-modulation of *PCDH-PC*, NSE, and *TUBB3* and increased expression of active phosphorylated Akt, p53, and *MYC*. Together, these observations further qualified *PCDH-PC* as a novel *in vitro* marker of NE differentiation in PCa cells and indicate that its expression may fluctuate in concordance with AR activity. After more than 11 months of culturing, the obtained LNCaP derivative grows perfectly in androgen-depleted media and expresses significant levels of AR and PSA. The growth rate was comparable to cultures of parental LNCaP cells grown in normal media (Figure W1*C*). For subsequent studies, these cells will be referred to as LNCaP–androgen-independent (LNCaP-AI).

The Androgen/AR Axis Regulates PCDH-PC *Expression*

We then sought to determine the extent to which the androgen/AR axis regulates *PCDH-PC* expression. LNCaP were treated during 24 hours with increasing concentrations of the androgen DHT, and *KLK3* (PSA) and *PCDH-PC* mRNA levels were measured by qRT-PCR. The increased level of *KLK3*, an AR-targeted gene, was used as a positive control of the AR activity in the presence of DHT. In DHT-treated cells, we observed a four-fold reduction in *PCDH-PC* mRNA levels in conjunction with increased *KLK3* expression (Figure 2*A*). The temporal effects of androgen were further tested in an experiment where the cells were maintained in androgen-depleted media for 72 hours and then DHT was added back for 6, 12, and 24 hours. In such conditions, inhibition of PCDH-PC expression was detectable as early as 6 hours following DHT supplementation, suggesting that the androgen/AR axis directly mediates PCDH-PC expression (Figure 2*B*).

Moreover, PCDH-PC expression was similarly reduced when cells were chronically exposed to androgens (Figure W2*A*), estrogen, or progesterone, which are two alternative ligands of mutated AR in this line [25]. We then asked whether a functional AR is required to mediate the repressive effect of androgens on *PCDH-PC* expression. LNCaP cells were incubated in the presence of the antiandrogen bicalutamide [26]. A 10-day treatment resulted in augmenting by seven-fold *PCDH-PC* expression (Figure 2*C*) while expectedly reducing *KLK3* expression. Changes in cell morphology were also visible upon the treatment (Figure W2*B*). We next applied bicalutamide treatment to the LNCaP-AI derivative. We observed a dose-dependent relative decrease in *KLK3* and *KLK2* expression compared to untreated cells with a concurrent increase in *PCDH-PC* expression (Figure 2*D*). To ascertain our assumption that *PCDH-PC* is repressed by AR activity, we next treated

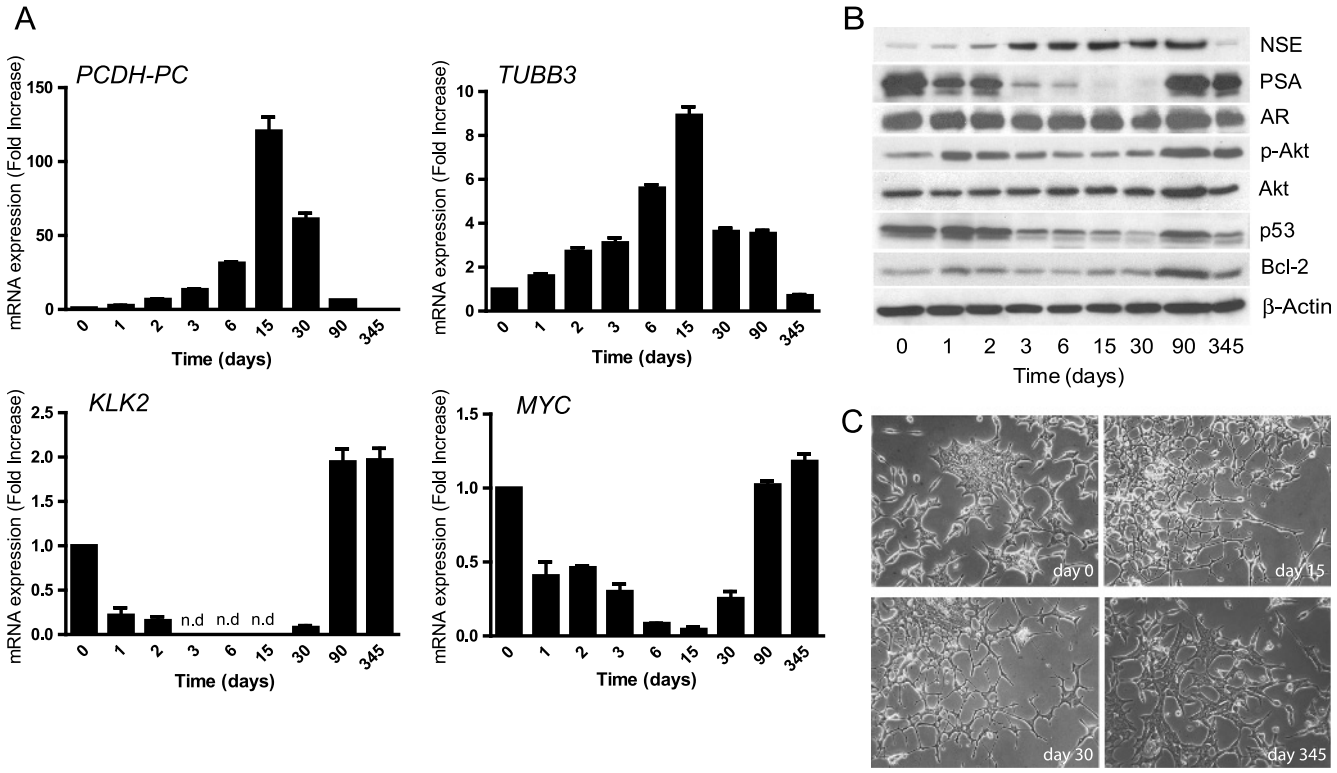

Figure 1. Phenotypic changes in LNCaP cells upon long-term androgen deprivation. At day 0, monolayer cultures of LNCaP cells were grown in 10% CS-FBS–containing medium. (A) qRT-PCR analysis for mRNA expression of *PCDH-PC*, *TUBB3*, *KLK2*, and *MYC*. (B) Western blot analysis for indicated proteins. β-Actin is used as a loading control. Densitometry of some western blot bands is provided in Figure W1*A*. (C) Morphology of cultured LNCaP cells maintained in medium containing 10% FBS (day 0) or 10% CS-FBS–containing medium for 15, 30, or 345 days. Photomicrographs are taken at ×10 objective magnification under inverted light microscopy.

the LNCaP-AI cells with docetaxel. Docetaxel is the standard-of-care first-line chemotherapy for men with metastatic CRPC. In PCa cells, recent studies showed that short-term treatment with docetaxel impeded AR activity [27]. Here, we exposed LNCaP-AI cells to 2.5 nM docetaxel for a prolonged period and examined the expression of *PCDH-PC* and NE markers over time. After 15 days, we found that the cell populations surviving this chronic exposure to docetaxel had greater levels of NE markers *NSE* (~2- to 4-fold increase), *TUBB3* (~2- to 5-fold increase), and *PCDH-PC* (~25- to 125-fold increase) compared to untreated cells (Figure 2*E*). The morphology of the cells also changed substantially with the formation of neurite outgrowths (Figure 2*F*). These data suggest that NE-like cancer cells likely emerged through transdifferentiation following the chronic exposure to docetaxel.

PCDH-PC Is a Negative Mediator of Ligand-Dependent AR Transcriptional Activity

We earlier found that transient overexpression of *PCDH-PC*, under certain circumstances, can perturb AR protein stability in LNCaP cells through a complex mechanism that involves Akt activation and increase proteasomal activity toward AR [28]. However, the potential links between AR activity, *PCDH-PC* expression, and phenotypic changes in LNCaP cells have not been investigated. Here, we tested the possibility that *PCDH-PC* expression could disrupt androgen signaling. We transiently overexpressed *PCDH-PC* using cultures of LNCaP cells. Increased expression of *PCDH-PC* was verified by qRT-PCR (Figure W3*A*); Western blot analysis showed a marked down-regulation of PSA in PCDH-PC–transfected cells while expectedly increased NSE and phospho-Akt levels (Figure 3*A*). There was also significant enrichment for inactivated phospho–glycogen synthase kinase-3 beta (GSK-3β; Ser9). The AR level was not perturbed, suggesting that *PCDH-PC* expression disrupted androgen signaling by inhibition of AR activity in our conditions. To further explore this inhibitory effect, we performed luciferase reporter assays on these latter cells following transfection of incremental amounts of the *PCDH-PC* expression construct. These analyses demonstrated a dose-dependent decrease of the PSA promoter transactivation (Figure 3*B*). We then investigated long-term effects of *PCDH-PC* expression by analyzing PSA expression in LNCaP derivatives stably transfected with *PCDH-PC*. In normal culture conditions, these cells showed more neurites and a decrease in cell growth compared to control cells (Figure 3*C*). PCDH-PC mRNA and protein levels in LNCaP-pcDNA3 and LNCaP–PCDH-PC are depicted in Figure W3, *B* and *C*. Stable transfectants exhibited reduced AR activity compared to vector-transfected LNCaP cells (Figure 3*D*). These cells have enhanced levels of endogenous NSE, phospho-Akt, and phospho–GSK-3β, comparable AR expression, but lower levels of PSA protein compared to the vector-transfected or LNCaP-AI cells (Figure 3*E*). Interestingly, inhibition of phosphatidylinositol 3-kinase (PI3K)/Akt signal using the PI3K inhibitor LY294002 compromised NE features in these cells (Figure 3*F*). We next investigated whether knockdown of PCDH-PC could affect the AR activity in the 22Rv1 PCa cells [29], which endogenously express *PCDH-PC*. 22Rv1 cells are androgen-independent given that they can grow in the absence of androgens. However, they remain AR dependent expressing several AR target genes including *KLK3* and *KLK2*. When 22Rv1 cells were maintained in the presence of androgens, ablation of *PCDH-PC* with *PCDH-PC*–targeted siRNAs did not significantly affect *KLK3* expression (Figure 3*G*). By contrast, this led

to *KLK2* levels that were approximately 12-fold higher. It was earlier demonstrated that 22Rv1 is androgen responsive for *KLK2* but weakly for *KLK3* expression [30]. We confirmed this information in an experiment where cells were exposed to 10 nM DHT for 24 hours (Figure 3*H*). Thus, we conceived that *PCDH-PC* is a potential repressor of ligand-dependent AR activity in this line. To pursue this possibility, we transiently transfected 22Rv1 cells with a PCDH-PC expression construct or control vector and measured *KLK2* and *KLK3* in either control (ethanol) or DHT-treated cells. Overexpression of *PCDH-PC* resulted in a significant decrease in *KLK2* expression compared to minor changes

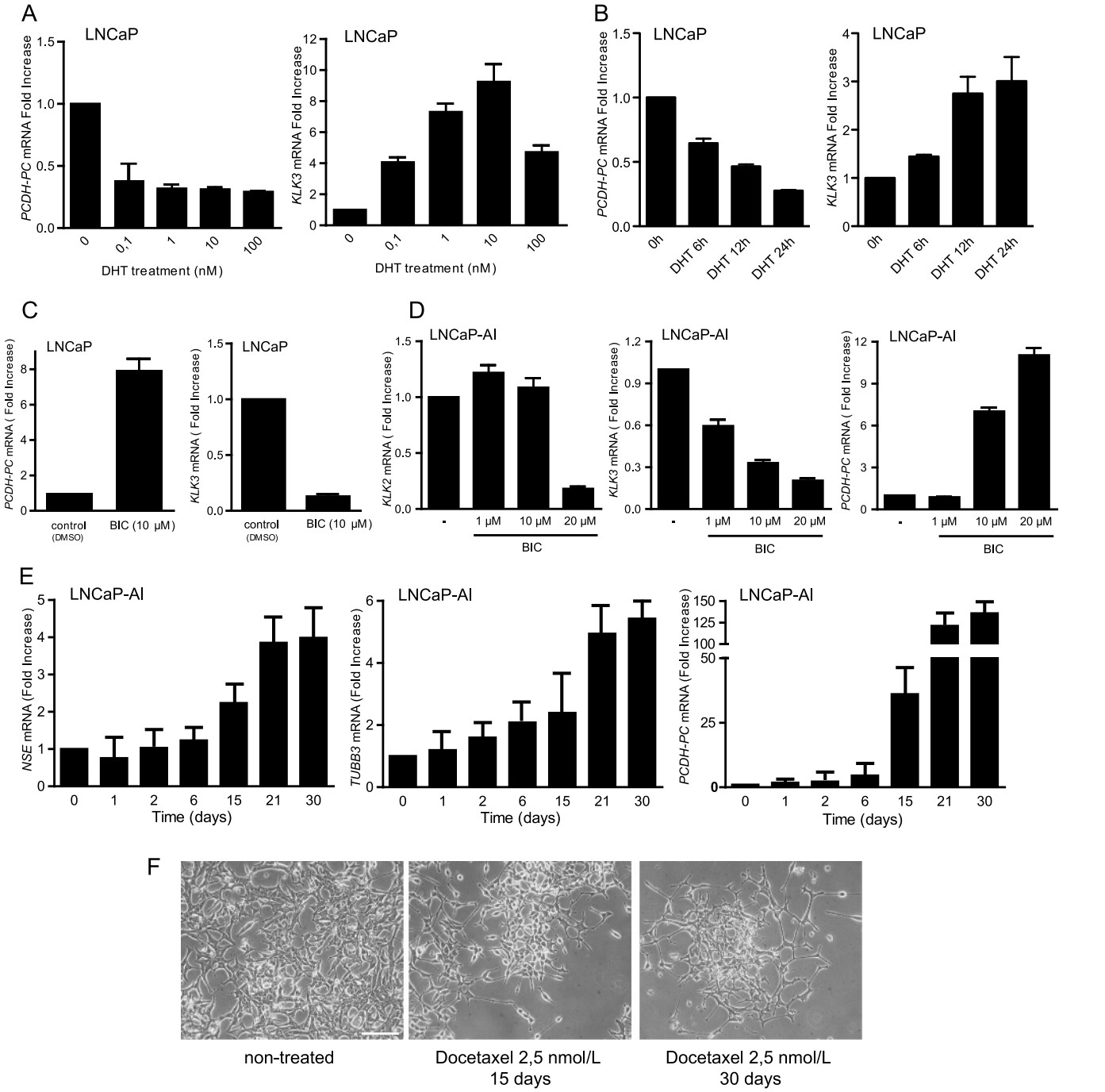

Figure 2. Androgenic regulation of the *PCDH-PC* gene. (A) Cultures of LNCaP cells were grown 24 hours in 10% CS-FBS media supplemented or not with incremental doses of DHT. RT-PCR analysis for *PCDH-PC* (left) and *KLK3* (right) levels in DHT-treated over vehicle-treated cells. (B) LNCaP cells were grown for 72 hours in 5% CS-FBS media and then refreshed with media supplemented with 100 nM DHT, and *PCDH-PC* and *KLK3* levels were inspected at the indicated times. (C) LNCaP cells were grown in 10% FBS in the presence or absence of bicalutamide (10 μM) for 10 days, and mRNA levels for *PCDH-PC* and *KLK3* were examined. (D) Histograms showing normalized levels of *KLK2* (left), *KLK3* (middle), and *PCDH-PC* (right) from LNCaP-AI cultures treated with bicalutamide for 8 days. (E) Time course expression of *NSE* (left), *TUBB3* (middle), and *PCDH-PC* (right) in LNCaP-AI cells cultivated at 2.5 nM docetaxel. Bars represent means ± SEM of two independent experiments done in triplicate. (F) Morphology of LNCaP-AI cells maintained in medium containing 10% CS-FBS (left panel), supplemented with docetaxel for 15 days (middle) or 30 days (right). Scale bar, 200 μm.

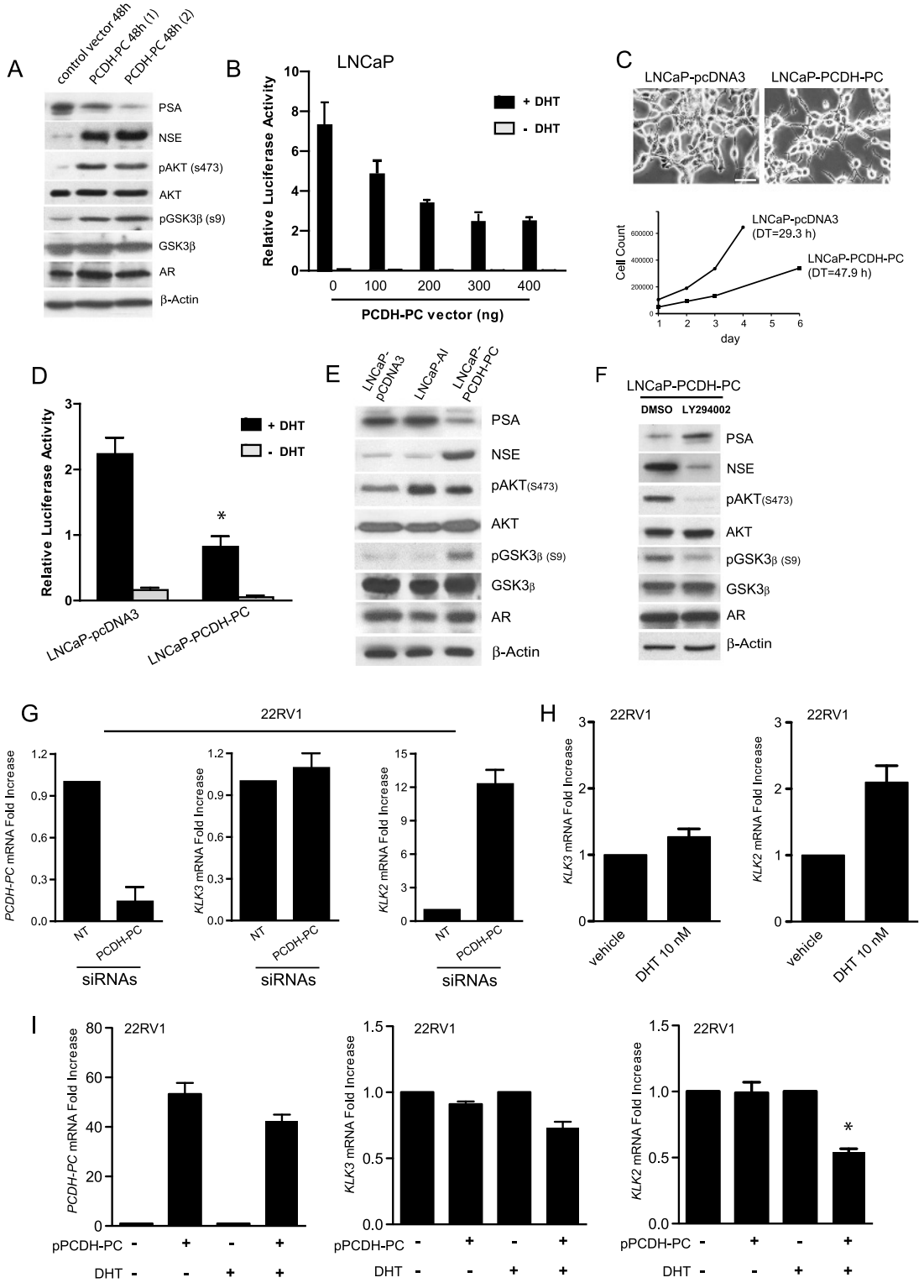

Figure 3. *PCDH-PC* expression reduces ligand-bound AR activity. (A) Western blot analysis 48 hours following transient transfection of *PCDH-PC* cDNA or the control vector. (B) PSA promoter activity was assessed in transfected LNCaP cells by measuring luciferase activity 24 hours after DHT treatment in cellular extracts normalized to β-Gal activity. (C) Stable transfectants of vector- and PCDH-PC–transfected LNCaP (LNCaP–PCDH-PC) were examined for differences in cell morphology and cell growth (DT), and PSA promoter activity (D) as in B. (E) Western blot made against proteins from LNCaP-pcDNA3, LNCaP-AI, and LNCaP–PCDH-PC cells showing reduced PSA and increased levels of NSE in the LNCaP–PCDH-PC cells. (F) LNCaP–PCDH-PC cells were treated for 3 days with either the PI3K inhibitor LY294002 (10 μM) or vehicle (DMSO). A Western blot was performed and probed as above. (G) 22Rv1 cells transfected either with siRNAs raised against PCDH-PC mRNA or non-targeting siRNA were analyzed for mRNA expression of *PCDH-PC*, *KLK3*, and *KLK2*. Down-regulation of *PCDH-PC* is accompanied by elevation of *KLK2* mRNA but had minor effects on *KLK3*. (H) 22Rv1 cells were treated with vehicle (EtOH) or DHT (10 nM) for 24 hours, and endogenous levels of *KLK3* and *KLK2* were examined. (I) 22Rv1 cells pretransfected with PCDH-PC plasmid were treated with vehicle (EtOH) or DHT (10 nM) for 24 hours, and *PCDH-PC*, *KLK3*, and *KLK2* levels were compared by qPCR.

for *KLK3* (Figure 3*I*), and the effect was perceived only in the presence of DHT. Together, these results strongly suggest that PCDH-PC overexpression inhibits ligand-dependent activity of AR in PCa cells, with no or marginal effects on its ligand-independent activity.

PCDH-PC Expression during PCa Progression

By immunohistochemistry, we then explored the distribution of PCDH-PC protein in normal and pathologic specimens. In tissues derived from normal prostate, luminal epithelial cells were consistently found to be negative for PCDH-PC and pronounced expression of this protein was observed in lonely cells scattered within the epithelium (Figure 4*A*, i). Occasionally, a faint staining was detected in the basal cell layer (Figure W4). A series of HNPC specimens was examined using tissue microarrays. This analysis revealed moderate to high expression of PCDH-PC in at most 11% (25 of 222) of evaluable cases (Table 1). There was no significant correlation with clinicopathologic data (Table W3). Evaluation of PCDH-PC expression in CRPC samples indicated a much higher proportion of positive cases (that is, 61%, 33 of 54 CRPC; Figure 4*A*, ii and Table 1). It is noteworthy that PCDH-PC protein was also detectable in cancer cells of metastatic CRPC lesions present in the brain and the lymph nodes of patients (Figure 4*A*, iii–iv). Despite only six cases were analyzed, this suggested that deregulated expression of PCDH-PC in CRPC is not restricted to recurrent lesions localized to the prostate.

We then evaluated a series of prostatectomy specimens of PCa obtained from patients treated for 3 to 6 months with neoadjuvant hormone therapy (HTPC). Of the 32 cases of HTPC evaluated, 14 (43.7%) were recorded as positive for PCDH-PC (Table 1).

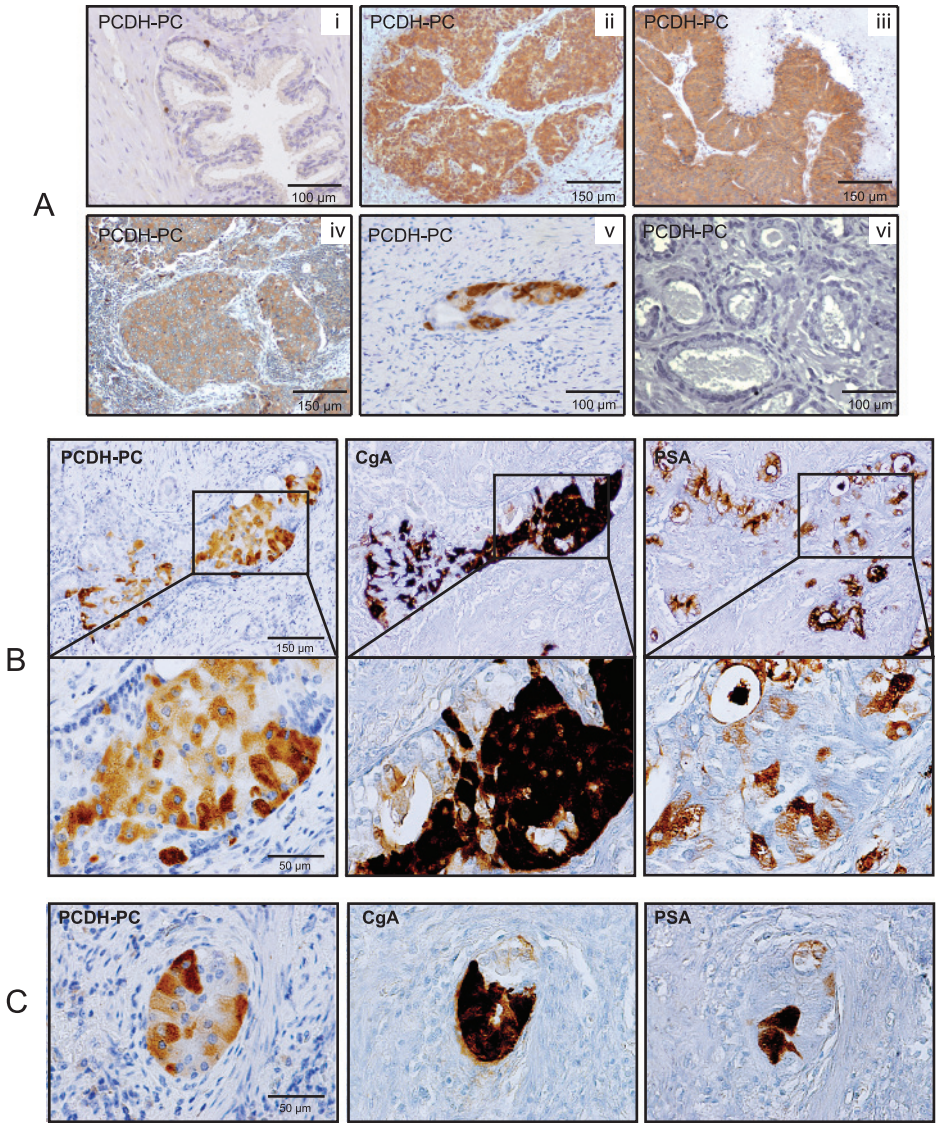

Figure 4. (A) Expression of PCDH-PC in human prostatic tissues. Anti–PCDH-PC identifies single normal cells in the prostatic epithelium of a healthy subject (i), in PCa cells in prostate tissue of CRPC (ii), in brain containing PCa metastases (iii), and in a lymph node metastasis (iv) of CRPC. (v) Positive PCDH-PC staining in cancer cells of a section of the surgical piece from a patient who had received 3 months of neoadjuvant ADT. (vi) Representative biopsy core from the same patient before neoadjuvant ADT showing negativity for PCDH-PC. (B, C) Expression of PCDH-PC correlates with NE characteristics in human PCa. Representative consecutive sections stained with antibodies to PCDH-PC, CgA, and PSA of primary PCa from a patient treated by neoadjuvant ADT. Immunohistochemical stains reveal mixed populations of cancer cells suggesting a common origin.

Table 1. PCDH-PC Expression before and after ADT.

Prostate Carcinoma	No. of PCDH-PC–Negative Samples (%)		No. of PCDH-PC–Positive Samples (%)
HNPC	197 (88.8)		25 (11.2)
HTPC	18 (56.3)		14 (43.7)
CRPC	21 (38.9)		33 (61.1)
Pearson χ^2 test		$P < .0001$	
Fisher exact test			
HNPC/HTPC		$P < .0001$	
HTPC/CRPC		$P = .178$	
HNPC/CRPC		$P < .0001$	

Especially, intense expression was consistently detected in clusters comprising of 5 to 100 cells (Figure 4*A*, v). For the overall HTPC group, PCDH-PC was found to be significantly higher when compared with the HNPC group as evaluated by Fisher exact test ($P < .0001$). To test further the hypothesis that ADT is causative for increased expression of PCDH-PC in these specimens, we examined the hormone-naïve tissues of these patients by examining their initial prostatic biopsies. Matched biopsy specimens were available in seven cases. In six of these index cases, we found no evidence of PCDH-PC expression after analyzing cancer foci of several biopsy specimens (Figure 4*A*, vi), and one other case showed strong positivity for PCDH-PC but in dispersed isolated cells rather than in clusters. These results demonstrate that high PCDH-PC expression is rare in men with still hormonally untreated PCa but substantially increases in response to hormonal manipulation.

PCDH-PC Expression Associates with NE Features in Human Prostate Tissues

Given the apparent link between PCDH-PC and NE features *in vitro*, we explored the value of PCDH-PC as a novel candidate marker for NE transdifferentiation in human PCa specimens. Examination of the hormone-treated samples for CgA and PSA expressions consistently revealed that cancer cells expressing PCDH-PC are present in tumor foci showing a large majority of CgA-expressing cells but with reduced expression of PSA (Figures 4, *B* and *C*, 5*A*, and W5*A*). Dual immunofluorescence procedure also revealed that in these tumor areas, not all cells exhibited the same NE characteristics such that varied levels of NE markers were observed in the cells (Figure 5*B*). In adjacent benign epithelia, we detected a few isolated cells staining positive for both CgA and PCDH-PC likely representing nonmalignant NE cells (Figure W5*B*).

On further analysis of cancer foci positive for PCDH-PC, we found positivity for the AR as well as for NSE and synaptophysin,

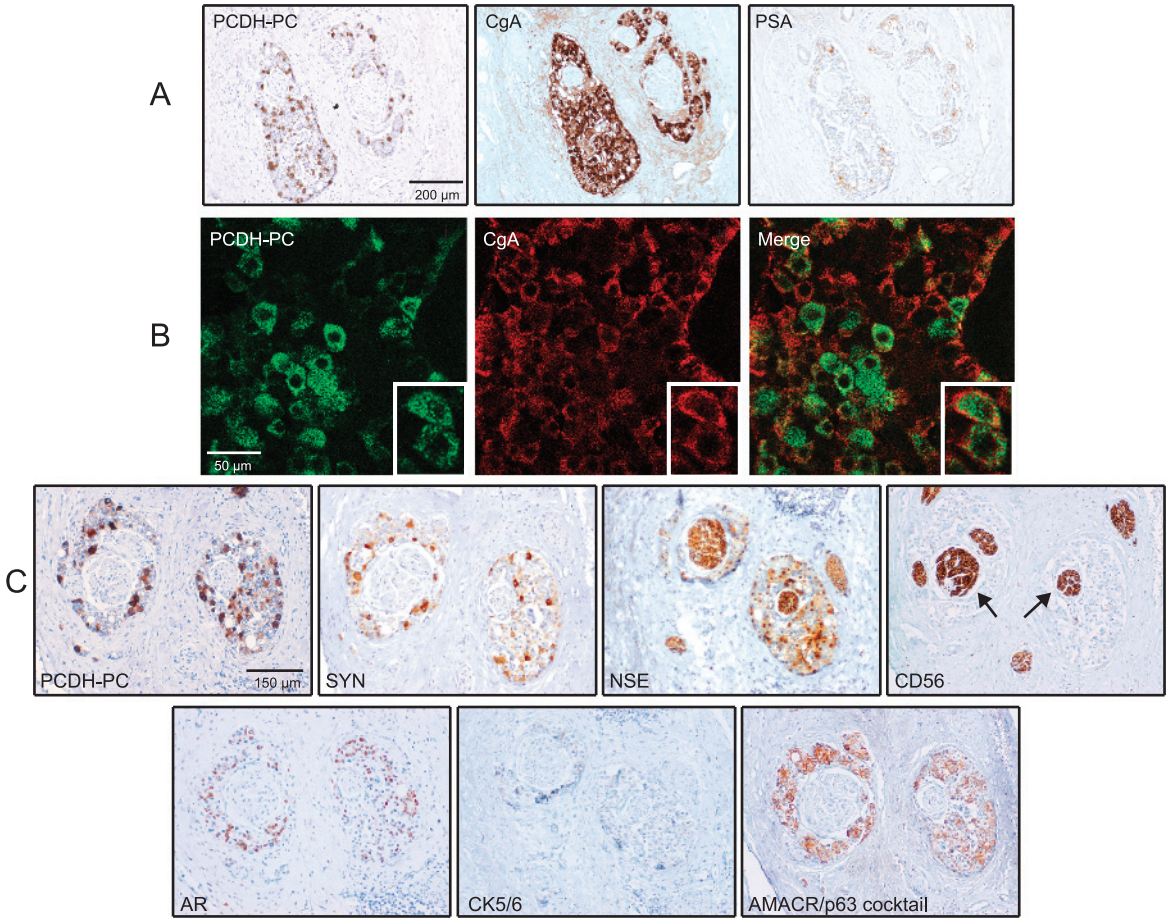

Figure 5. (A) Immunohistochemical analysis further validating the inverse correlation between PCDH-PC/CgA stainings and PSA expression in tumor foci of a hormonally treated case. (B) Dual immunofluorescence in the previous index case identifies cancer cells coexpressing PCDH-PC and CgA. The cells can express varied levels of the two proteins. (C) A positive PCDH-PC cancer focus was analyzed for expression of synaptophysin (SYN), NSE, N-CAM (CD56), AR, basal cytokeratins 5/6, AMACR, and p63. Note the areas positive for NSE and CD56 (arrows) but negative for the other markers representing nontumoral nerves present in the prostate tissue.

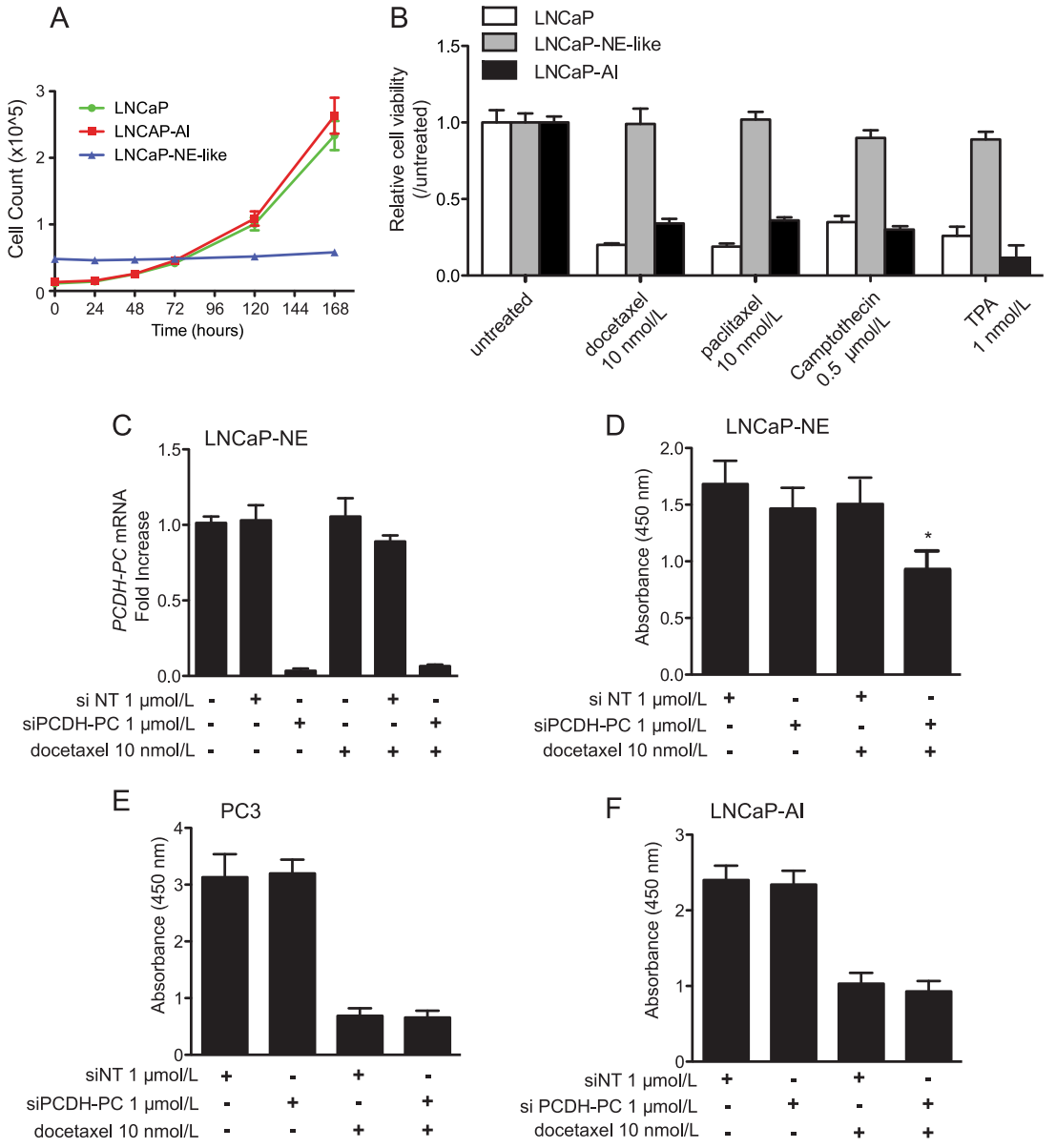

Figure 6. Acquired NE phenotype correlates with chemoresistance in LNCaP cells. (A) LNCaP, LNCaP-NE like, and LNCaP-AI derivatives were examined for differences in cell growth. (B) Viability assay of LNCaP (white bars), LNCaP–NE-like (gray bars), and LNCaP-AI (black bars) cells at 96 hours after treatment with docetaxel, paclitaxel, camptothecin, or phorbol ester (TPA) relative to untreated cells. (C) Verification of efficient *PCDH-PC* knockdown by qRT-PCR in LNCaP–NE-like cells pretreated 24 hours with either Accell Non-Targeting or PCDH11Y siRNAs and then maintained in the presence or absence of docetaxel for 48 hours. (D) Cell viability as assessed by WST-1 assay using siRNAs treated with LNCaP–NE-like cells alone or subsequently treated with docetaxel for 8 days. (E) As in C except using PC3 cells and 96-hour docetaxel treatment. (F) As in D except using LNCaP-AI cells. Bars represent means ± SEM of quintuplets from one experiment representative of three independent experiments.

two established NE markers, but we consistently failed to detect staining for CD56 (NCAM1; Figure 5*C*), another NE marker. Of note, cancer areas within the different tissues analyzed (PCDH-PC positive and negative) were consistently negative for the Ki67 antigen (not shown). Moreover, PCDH-PC–expressing cells were negative for the basal cytokeratins 5/6 and p63 but positive for α-methylacyl-CoA racemase (AMACR; Figure 5*C*), a highly specific marker of PCa epithelia, thus supporting a PCa origin [31].

Collectively, these observations strongly suggest PCDH-PC as a novel early marker for transition from epithelial to NE phenotype in PCa treated by ADT. Intriguingly however, at the castration state of prostate adenocarcinoma, the relationship between PCDH-PC expression and NE (as assessed by CgA staining) appeared to be lost, and although PCDH-PC immunostaining of PCa cells sometimes coincides with staining for NE markers such as NSE (Figure W5*C*), in many cases the PCDH-PC–positive contingents examined did not show coincidental staining (not shown).

NE-like PCa Cells Are Resistant to Chemotherapeutic Agents

Several pieces of evidence suggest that PCa NE-like cells are resistant to multiple therapeutics agents [32,33]. Here, we assessed further the

chemoresistance spectrum of LNCaP–NE-like cells. After culturing LNCaP cells for 15 days in androgen-depleted medium, the cells exhibit an NE-like phenotype and reduced growth (Figure 6*A*) concomitant with a loss of their epithelial characteristics. Sensitivity with respect to diverse agents was evaluated 96 hours after treatment of LNCaP–NE-like, LNCaP, or LNCaP-AI cells. Treatments included two taxanes, docetaxel and paclitaxel, as well as 12-O-tetradecanoylphorbol-13-acetate (TPA) and camptothecin, two well-known inducers of apoptosis in LNCaP cells [34,35]. At the indicated doses, LNCaP–NE-like cells were overwhelmingly resistant to these drugs compared to LNCaP or LNCaP-AI cells (Figure 6*B*). LNCaP–NE-like cells also showed enhanced resistance to various cytotoxic agents commonly used in management of various malignancies (Figure W6*A*). We next wanted to gauge the dependence of LNCaP–NE-like cells with respect to PCDH-PC expression for their viability. To this end, LNCaP–NE-like cells were treated for 24 hours with Accell Green Non-Targeting siRNAs used to control effective uptake of the siRNAs (Figure W6*B*), pools of Accell Non-Targeting siRNAs, or Accell siRNAs raised against PCDH-PC transcripts, then cultured for 8 days in hormone-deprived medium supplemented or not with docetaxel (10 nM). PCDH-PC silencing was found to be efficient in these conditions (Figure 6*C*). In the presence of docetaxel, LNCaP-NE cells that had been preincubated with the PCDH-PC siRNAs showed a significant decrease in cell viability (relative to cells exposed to NT siRNA in the presence or absence of docetaxel), whereas in the absence of docetaxel, PCDH-PC siRNA treatment had limited effect (Figure 6*D*). Moreover, the effect was not seen when similar treatments were applied to the chemosensitive PC3 PCa lineage (Figure 6*E*), which lacks *PCDH-PC* or LNCaP-AI that expresses low amounts of *PCDH-PC* (Figure 6*F*). Subsequent analyses showed that attenuating PCDH-PC expression similarly sensitized LNCaP–NE-like cells to TPA and camptothecin (Figure W6, *C* and *D*). These data argue for a chemoprotective role for PCDH-PC in LNCaP–NE-like cells.

Discussion

The androgen/AR axis remains active in the majority of CRPCs. However, as prostate tumors develop resistance to treatment, NE differentiation has been proposed as a mechanism for hormonal escape or AR independence [4,10–12,36–38]. Yet, the impact of NE differentiation on the clinical outcome, the mechanisms by which NE differentiation emerges after ADT, and the consequence of targeting these cell populations remain uncertain. The current study significantly expands our understanding of NE differentiation in PCa and qualifies PCDH-PC as a surrogate marker for human PCa cell subpopulations experiencing NE transdifferentiation under hormonal treatment.

With respect to progression toward a castration-resistant phenotype, results obtained from LNCaP cultures grown in androgen-reduced medium support a model in which AR function is attenuated in a first phase following ADT, concomitantly with the acquisition of NE features by PCa cells. *In situ*, we found evidence that high PCDH-PC expression also parallels CgA and other NE markers in clusters of tumor cells from neoadjuvant hormonally treated PCa. The fact that normal NE cells are considered as post-mitotic [39], coupled with data showing that the proliferating rate of PCa cells is relatively low in primary prostate tumors [40], strongly suggests that NE-like clusters revealed in this study originated from the NE transdifferentiation of preexisting epithelial-looking PCa cells. Thus, we propose that in clinical setting, overexpression of PCDH-PC and concomitant induction of NE transdifferentiation by a fraction of PCa cells in early response to hormonal treatment reflects one route for PCa cells to adapt and survive in a low androgen environment.

In a second step, AR may be reactivated [5,41,42] to promote proliferation in conjunction with partial or total loss of NE features along with reappearance of significant amounts of PSA as observed in LNCaP-AI cells. Further studies are warranted to decrypt the mechanisms involved in reactivation of AR in these cells.

Enigmatically, the relationship between PCDH-PC and NE differentiation was not evident in CRPC specimens. This could reflect the multifaceted role of PCDH-PC in the more advanced stages of PCa with functions that may occur independently of NE differentiation. Alternatively, this could be indicative of various subtypes of NE differentiation (from well differentiated to poorly differentiated) in tumors with varied proliferative activity and expressing various levels of NE markers [43,44]. In that respect, it will be important to examine the role of PCDH-PC in the setting of small cell carcinoma of prostate, a rare poorly differentiated NE PCa associated with poor prognosis and poor response to therapies [45]. It is also tempting to speculate that AR plays a crucial role in this potential molecular switch as AR is consistently implicated in the growth of castrate-resistant tumors [41,46]. We have shown here that PCDH-PC expression inhibits AR activity. However, this inhibition appeared to be incomplete in the sense that it is likely restricted to the ligand-dependent activity of AR. Although we already know that PI3K/Akt activity may be an important mediator of this effect, the precise mechanism through which PCDH-PC regulates the ligand-dependent AR activity has yet to be fully determined.

If confirmed, this regulation could also indicate that among castrate-resistant tumors, those overexpressing PCDH-PC might progress to the favor of tumor clones dependent on a ligand-independent activity of AR [46–48].

Our experimental data consistently revealed that androgen exposure inhibits PCDH-PC expression in LNCaP cells, although it is unlikely that androgens completely switch off PCDH-PC expression. Likewise, the contribution of other recurrent alterations found in PCa, such as *TMPRSS2-ERG* gene fusion or loss of PTEN, known to perturb AR signaling, should be considered [49,50].

Another interesting observation is that the NE status of LNCaP cells correlates with resistance to a wide range of chemotherapeutic agents including docetaxel, the current standard for metastatic CRPC. One could suggest that those resistances are likely linked to the reduced growth rate of LNCaP–NE-like cells. Indeed, from a clinical perspective, the observation that NE transdifferentiation could confer a multidrug-resistant phenotype allowing a cell to remain arrested until it can reacquire the ability to proliferate could make that process a formidable tumor promoter at any stage of PCa progression. Interestingly, by targeting NE-like PCa cells using RNA interference against PCDH-PC, it was possible to sensitize cells to chemohormonal treatment. Together with prior work identifying PCDH-PC as an anti-apoptotic factor in PCa cells [13], this qualifies PCDH-PC as a general survival factor in PCa cells and provides a biologic rationale for further assessment of targeting malignant NE-like cells.

Although not emphasized here, in neoadjuvant hormonally treated tumors, we found many instances with NE-like PCa (PCDH-PC$^+$, CgA$^+$, PSA$^-$) cells adjacent to malignant epithelial-like (PCDH-PC$^-$, CgA$^-$, PSA$^+$) cells, thus continuing to use the androgen/AR axis despite ADT (Figure 4). Clearly, the manifestation of these mixed populations gives reason to further examine whether these phenotypically distinct cell populations may cooperate to promote transition toward castration

resistance [8,51], which would either help support or refute a rationale of treating both adenocarcinoma and NE components.

In summary, our study provides support for the likelihood of transdifferentiation model of PCa cells to explain the emergence of NE differentiation in human PCa following ADT. We substantiate PCDH-PC, a human male-specific protocadherin, as a critical factor in this process that appears to be regulated by cross modulation between PCDH-PC and AR. Along this line, our data revealed novel paradigms linking the AR axis and NE transdifferentiation in PCa cells with apparent implications for the emergence of chemohormonal resistance.

Acknowledgments

We are grateful to Ralph Buttyan (Vancouver Prostate Centre) for advice and critical reading of this work. We are also grateful to Fannie Semprez, Luis Queires, Renée Delbé, and Noëmie Lemenand for technical support critical to this work.

References

[1] Siegel R, Naishadham D, and Jemal A (2012). Cancer statistics, 2012. *CA Cancer J Clin* **62**, 10–29.

[2] Isaacs JT and Isaacs WB (2004). Androgen receptor outwits prostate cancer drugs. *Nat Med* **10**, 26–27.

[3] Denmeade SR and Isaacs JT (2002). A history of prostate cancer treatment. *Nat Rev Cancer* **2**, 389–396.

[4] Beltran H, Beer TM, Carducci MA, de Bono J, Gleave M, Hussain M, Kelly WK, Saad F, Sternberg C, Tagawa ST, et al. (2011). New therapies for castration-resistant prostate cancer: efficacy and safety. *Eur Urol* **60**, 279–290.

[5] Feldman BJ and Feldman D (2001). The development of androgen-independent prostate cancer. *Nat Rev Cancer* **1**, 34–45.

[6] Burchardt T, Burchardt M, Chen MW, Cao Y, de la Taille A, Shabsigh A, Hayek O, Dorai T, and Buttyan R (1999). Transdifferentiation of prostate cancer cells to a neuroendocrine cell phenotype *in vitro* and *in vivo*. *J Urol* **162**, 1800–1805.

[7] Wright ME, Tsai MJ, and Aebersold R (2003). Androgen receptor represses the neuroendocrine transdifferentiation process in prostate cancer cells. *Mol Endocrinol* **17**, 1726–1737.

[8] Yuan TC, Veeramani S, Lin FF, Kondrikou D, Zelivianski S, Igawa T, Karan D, Batra SK, and Lin MF (2006). Androgen deprivation induces human prostate epithelial neuroendocrine differentiation of androgen-sensitive LNCaP cells. *Endocr Relat Cancer* **13**, 151–167.

[9] Sauer CG, Roemer A, and Grobholz R (2006). Genetic analysis of neuroendocrine tumor cells in prostatic carcinoma. *Prostate* **66**, 227–234.

[10] Cindolo L, Cantile M, Vacherot F, Terry S, and de la Taille A (2007). Neuroendocrine differentiation in prostate cancer: from lab to bedside. *Urol Int* **79**, 287–296.

[11] Jiborn T, Bjartell A, and Abrahamsson PA (1998). Neuroendocrine differentiation in prostatic carcinoma during hormonal treatment. *Urology* **51**, 585–589.

[12] di Sant'Agnese PA (1992). Neuroendocrine differentiation in human prostatic carcinoma. *Hum Pathol* **23**, 287–296.

[13] Chen MW, Vacherot F, De La Taille A, Gil-Diez-De-Medina S, Shen R, Friedman RA, Burchardt M, Chopin DK, and Buttyan R (2002). The emergence of protocadherin-PC expression during the acquisition of apoptosis-resistance by prostate cancer cells. *Oncogene* **21**, 7861–7871.

[14] Blanco P, Sargent CA, Boucher CA, Mitchell M, and Affara NA (2000). Conservation of PCDHX in mammals; expression of human X/Y genes predominantly in brain. *Mamm Genome* **11**, 906–914.

[15] Yang X, Chen MW, Terry S, Vacherot F, Chopin DK, Bemis DL, Kitajewski J, Benson MC, Guo Y, and Buttyan R (2005). A human- and male-specific protocadherin that acts through the wnt signaling pathway to induce neuroendocrine transdifferentiation of prostate cancer cells. *Cancer Res* **65**, 5263–5271.

[16] Horoszewicz JS, Leong SS, Kawinski E, Karr JP, Rosenthal H, Chu TM, Mirand EA, and Murphy GP (1983). LNCaP model of human prostatic carcinoma. *Cancer Res* **43**, 1809–1818.

[17] Terry S, Queires L, Gil-Diez-de-Medina S, Chen MW, de la Taille A, Allory Y, Tran PL, Abbou CC, Buttyan R, and Vacherot F (2006). Protocadherin-PC promotes androgen-independent prostate cancer cell growth. *Prostate* **66**, 1100–1113.

[18] Cleutjens KB, van der Korput HA, van Eekelen CC, van Rooij HC, Faber PW, and Trapman J (1997). An androgen response element in a far upstream enhancer region is essential for high, androgen-regulated activity of the prostate-specific antigen promoter. *Mol Endocrinol* **11**, 148–161.

[19] Romijn JC, Verkoelen CF, and Schroeder FH (1988). Application of the MTT assay to human prostate cancer cell lines *in vitro*: establishment of test conditions and assessment of hormone-stimulated growth and drug-induced cytostatic and cytotoxic effects. *Prostate* **12**, 99–110.

[20] Beltran H, Rickman DS, Park K, Chae SS, Sboner A, MacDonald TY, Wang Y, Sheikh KL, Terry S, Tagawa ST, et al. (2011). Molecular characterization of neuroendocrine prostate cancer and identification of new drug targets. *Cancer Discov* **1**, 487–495.

[21] Terry S, Ploussard G, Allory Y, Nicolaiew N, Boissiere-Michot F, Maille P, Kheuang L, Coppolani E, Ali A, Bibeau F, et al. (2009). Increased expression of class III β-tubulin in castration-resistant human prostate cancer. *Br J Cancer* **101**, 951–956.

[22] van Steenbrugge GJ, van Uffelen CJ, Bolt J, and Schroder FH (1991). The human prostatic cancer cell line LNCaP and its derived sublines: an *in vitro* model for the study of androgen sensitivity. *J Steroid Biochem Mol Biol* **40**, 207–214.

[23] Chen M, Tanner M, Levine AC, Levina E, Ohouo P, and Buttyan R (2009). Androgenic regulation of hedgehog signaling pathway components in prostate cancer cells. *Cell Cycle* **8**, 149–157.

[24] Bernard D, Pourtier-Manzanedo A, Gil J, and Beach DH (2003). Myc confers androgen-independent prostate cancer cell growth. *J Clin Invest* **112**, 1724–1731.

[25] Veldscholte J, Berrevoets CA, Ris-Stalpers C, Kuiper GG, Jenster G, Trapman J, Brinkmann AO, and Mulder E (1992). The androgen receptor in LNCaP cells contains a mutation in the ligand binding domain which affects steroid binding characteristics and response to antiandrogens. *J Steroid Biochem Mol Biol* **41**, 665–669.

[26] Masiello D, Cheng S, Bubley GJ, Lu ML, and Balk SP (2002). Bicalutamide functions as an androgen receptor antagonist by assembly of a transcriptionally inactive receptor. *J Biol Chem* **277**, 26321–26326.

[27] Zhu ML, Horbinski CM, Garzotto M, Qian DZ, Beer TM, and Kyprianou N (2010). Tubulin-targeting chemotherapy impairs androgen receptor activity in prostate cancer. *Cancer Res* **70**, 7992–8002.

[28] Yang X, Chen MW, Terry S, Vacherot F, Bemis DL, Capodice J, Kitajewski J, de la Taille A, Benson MC, Guo Y, et al. (2006). Complex regulation of human androgen receptor expression by Wnt signaling in prostate cancer cells. *Oncogene* **25**, 3436–3444.

[29] Sramkoski RM, Pretlow TG II, Giaconia JM, Pretlow TP, Schwartz S, Sy MS, Marengo SR, Rhim JS, Zhang D, and Jacobberger JW (1999). A new human prostate carcinoma cell line, 22Rv1. *In Vitro Cell Dev Biol Anim* **35**, 403–409.

[30] Denmeade SR, Sokoll LJ, Dalrymple S, Rosen DM, Gady AM, Bruzek D, Ricklis RM, and Isaacs JT (2003). Dissociation between androgen responsiveness for malignant growth vs. expression of prostate specific differentiation markers PSA, hK2, and PSMA in human prostate cancer models. *Prostate* **54**, 249–257.

[31] Rubin MA, Zhou M, Dhanasekaran SM, Varambally S, Barrette TR, Sanda MG, Pienta KJ, Ghosh D, and Chinnaiyan AM (2002). α-Methylacyl coenzyme A racemase as a tissue biomarker for prostate cancer. *JAMA* **287**, 1662–1670.

[32] Deng X, Liu H, Huang J, Cheng L, Keller ET, Parsons SJ, and Hu CD (2008). Ionizing radiation induces prostate cancer neuroendocrine differentiation through interplay of CREB and ATF2: implications for disease progression. *Cancer Res* **68**, 9663–9670.

[33] Frigo DE and McDonnell DP (2008). Differential effects of prostate cancer therapeutics on neuroendocrine transdifferentiation. *Mol Cancer Ther* **7**, 659–669.

[34] Day ML, Zhao X, Wu S, Swanson PE, and Humphrey PA (1994). Phorbol ester-induced apoptosis is accompanied by NGFI-A and c-*fos* activation in androgen-sensitive prostate cancer cells. *Cell Growth Differ* **5**, 735–741.

[35] Akao Y, Kusakabe S, Banno Y, Kito M, Nakagawa Y, Tamiya-Koizumi K, Hattori M, Sawada M, Hirabayasi Y, Ohishi N, et al. (2002). Ceramide accumulation is independent of camptothecin-induced apoptosis in prostate cancer LNCaP cells. *Biochem Biophys Res Commun* **294**, 363–370.

[36] Shah RB, Mehra R, Chinnaiyan AM, Shen R, Ghosh D, Zhou M, Macvicar GR, Varambally S, Harwood J, Bismar TA, et al. (2004). Androgen-independent prostate cancer is a heterogeneous group of diseases: lessons from a rapid autopsy program. *Cancer Res* **64**, 9209–9216.

[37] Hirano D, Okada Y, Minei S, Takimoto Y, and Nemoto N (2004). Neuroendocrine differentiation in hormone refractory prostate cancer following androgen deprivation therapy. *Eur Urol* **45**, 586–592; discussion 592.

[38] Wafa LA, Palmer J, Fazli L, Hurtado-Coll A, Bell RH, Nelson CC, Gleave ME, Cox ME, and Rennie PS (2007). Comprehensive expression analysis of L-dopa decarboxylase and established neuroendocrine markers in neoadjuvant hormone-treated versus varying Gleason grade prostate tumors. *Hum Pathol* **38**, 161–170.

[39] Bonkhoff H, Stein U, and Remberger K (1995). Endocrine-paracrine cell types in the prostate and prostatic adenocarcinoma are postmitotic cells. *Hum Pathol* **26**, 167–170.

[40] Berges RR, Vukanovic J, Epstein JI, CarMichel M, Cisek L, Johnson DE, Veltri RW, Walsh PC, and Isaacs JT (1995). Implication of cell kinetic changes during the progression of human prostatic cancer. *Clin Cancer Res* **1**, 473–480.

[41] Chen CD, Welsbie DS, Tran C, Baek SH, Chen R, Vessella R, Rosenfeld MG, and Sawyers CL (2004). Molecular determinants of resistance to antiandrogen therapy. *Nat Med* **10**, 33–39.

[42] Heinlein CA and Chang C (2004). Androgen receptor in prostate cancer. *Endocr Rev* **25**, 276–308.

[43] Klimstra DS, Modlin IR, Adsay NV, Chetty R, Deshpande V, Gonen M, Jensen RT, Kidd M, Kulke MH, Lloyd RV, et al. (2010). Pathology reporting of neuroendocrine tumors: application of the Delphic consensus process to the development of a minimum pathology data set. *Am J Surg Pathol* **34**, 300–313.

[44] Helpap B and Kollermann J (2001). Immunohistochemical analysis of the proliferative activity of neuroendocrine tumors from various organs. Are there indications for a neuroendocrine tumor-carcinoma sequence? *Virchows Arch* **438**, 86–91.

[45] Wang W and Epstein JI (2008). Small cell carcinoma of the prostate. A morphologic and immunohistochemical study of 95 cases. *Am J Surg Pathol* **32**, 65–71.

[46] Sun S, Sprenger CC, Vessella RL, Haugk K, Soriano K, Mostaghel EA, Page ST, Coleman IM, Nguyen HM, Sun H, et al. (2010). Castration resistance in human prostate cancer is conferred by a frequently occurring androgen receptor splice variant. *J Clin Invest* **120**, 2715–2730.

[47] Dehm SM, Schmidt LJ, Heemers HV, Vessella RL, and Tindall DJ (2008). Splicing of a novel androgen receptor exon generates a constitutively active androgen receptor that mediates prostate cancer therapy resistance. *Cancer Res* **68**, 5469–5477.

[48] Hu R, Dunn TA, Wei S, Isharwal S, Veltri RW, Humphreys E, Han M, Partin AW, Vessella RL, Isaacs WB, et al. (2009). Ligand-independent androgen receptor variants derived from splicing of cryptic exons signify hormone-refractory prostate cancer. *Cancer Res* **69**, 16–22.

[49] Yu J, Yu J, Mani RS, Cao Q, Brenner CJ, Cao X, Wang X, Wu L, Li J, Hu M, et al. (2010). An integrated network of androgen receptor, polycomb, and TMPRSS2-ERG gene fusions in prostate cancer progression. *Cancer Cell* **17**, 443–454.

[50] Carver BS, Chapinski C, Wongvipat J, Hieronymus H, Chen Y, Chandarlapaty S, Arora VK, Le C, Koutcher J, Scher H, et al. (2011). Reciprocal feedback regulation of PI3K and androgen receptor signaling in PTEN-deficient prostate cancer. *Cancer Cell* **19**, 575–586.

[51] Jin RJ, Wang Y, Masumori N, Ishii K, Tsukamoto T, Shappell SB, Hayward SW, Kasper S, and Matusik RJ (2004). NE-10 neuroendocrine cancer promotes the LNCaP xenograft growth in castrated mice. *Cancer Res* **64**, 5489–5495.

Supplemental Experimental Procedures

Generation of Monoclonal Antibodies Specific for PCDH-PC

BALBc mice were immunized with a recombinant PCDH-PC expressed from an *Escherichia coli* (BL21-CodonPlus competent cells; Stratagene, Paris, France) transformed with a pET3a–PCDH-PC expression construct. After four repeats of immunization, mice splenocytes were fused using polyethylene glycol with X63 myeloma cells and grown in hypoxanthine-aminopterin-thymidine selection medium to generate hybridomas. After limit dilution, supernatants from hybridoma clones were screened for efficient detection of PCDH-PC using an ELISA procedure wherein recombinant PCDH-PC was coated on Immulon flat-bottom microtiter plates. Immunocytochemistry detection of PCDH-PC in the LNCaP–PCDH-PC was performed and compared to vector-transfected LNCaP cells to verify the specificity of the antibodies (Figure W3*C*). One hybridoma cell line designed "HB 0337 SSA" was selected for *in situ* detection of human PCDH-PC and deposited under No. I-3561 to the Collection Nationale de Cultures de Microorganismes, Institut Pasteur (Paris, France).

Table W1. List of Primary Antibodies Used.

Antibody	Source	Assay
PCDH-PC	Noncommercial* (HB 0337 SSA)	IHC
PSA	Dako (clone ER-PR8)	IHC
AMACR (P504S) + p63 (PIN cocktail)	Menarini Diagnostics (Rungis, France; polyclonal)	IHC
Chromogranin A	Dako (polyclonal)	IHC
TUBB3	Covance (Emeryville, CA; clone TUJ1)	IHC
AR	Dako (clone AR441)	IHC
NSE	Dako (clone BBS/NC/VI-H14)	IHC
Synaptophysin	Biogenex (San Ramon, CA; Snp88)	IHC
CD56	Dako (clone 123C3)	IHC
CK5/6	Dako (clone D5/16 B4)	IHC
AR	SC-AR441	WB
NSE	Millipore (Molsheim, France; MAB324)	WB
PSA	Dako (polyclonal)	WB
Akt	Cell Signaling Technology (Danvers, MA; polyclonal)	WB
Phospho-Akt (S473)	Cell Signaling Technology (polyclonal)	WB
GSK-3β	SC-9166	WB
Phospho–GSK-3β (S9)	Cell Signaling Technology (polyclonal)	WB
Bcl-2	Sigma (clone Bcl-2 100)	WB
β-Actin	Sigma (AC-15)	WB
p53	Dako (DO-7)	WB

IHC indicates immunohistochemistry.
*Available upon request.

Table W2. List of Primers Used.

Gene	Accession No.	Primer	qPCR Primer (5′-3′)
HMBS	NM_001024382	Forward	CCATCATCCTGGCAACAGCT
HMBS	NM_001024382	Reverse	GCATTCCTCAGGGTGCAGG
RPLP0	NM_001002	Forward	GGCGACCTGGAAGTCCAACT
RPLP0	NM_001002	Reverse	CCATCAGCACCACAGCCTTC
PPIA	NM_021130	Forward	ACCGTGTTCTTCGACATTGC
PPIA	NM_021130	Reverse	GGCATGAATATTGTGGAGGC
PCDH11Y (alias *PCDH-PC*)	NM_032971	Forward	AATTGGGTAACTACACCTACTA
PCDH11Y (alias *PCDH-PC*)	NM_032971	Reverse	CTCGAAGGTTGTCACTGGATA
TUBB3	NM_006086	Forward	GCCTCTTCTCACAAGTACGTG
TUBB3	NM_006086	Reverse	CCCCACTCTGACCAAAGATGAA
MYC	NM_002467	Forward	CTTCTCTCCGTCCTCGGATT
MYC	NM_002467	Reverse	CTCTGACCTTTTGCCAGGAG
KLK2	NM_005551	Forward	GCTGCCCATTGCCTAAAGAAG
KLK2	NM_005551	Reverse	TGGGAAGCTGTGGCTGACA
KLK3	NM_001648	Forward	GAGCACCCCTATCAACCCCCTATT
KLK3	NM_001648	Reverse	AGCAACCCTGGACCTCACACCTAA
NSE	NM_001975	Forward	CTGGCTAAATACAACCAGCTCA
NSE	NM_001975	Reverse	CACAGCACACTGGGATTACG
SHH	NM_000193	Forward	GGTATGCTCGGGACTGGCG
SHH	NM_000193	Reverse	CAGCCTGTCCGCTCCGGTGT

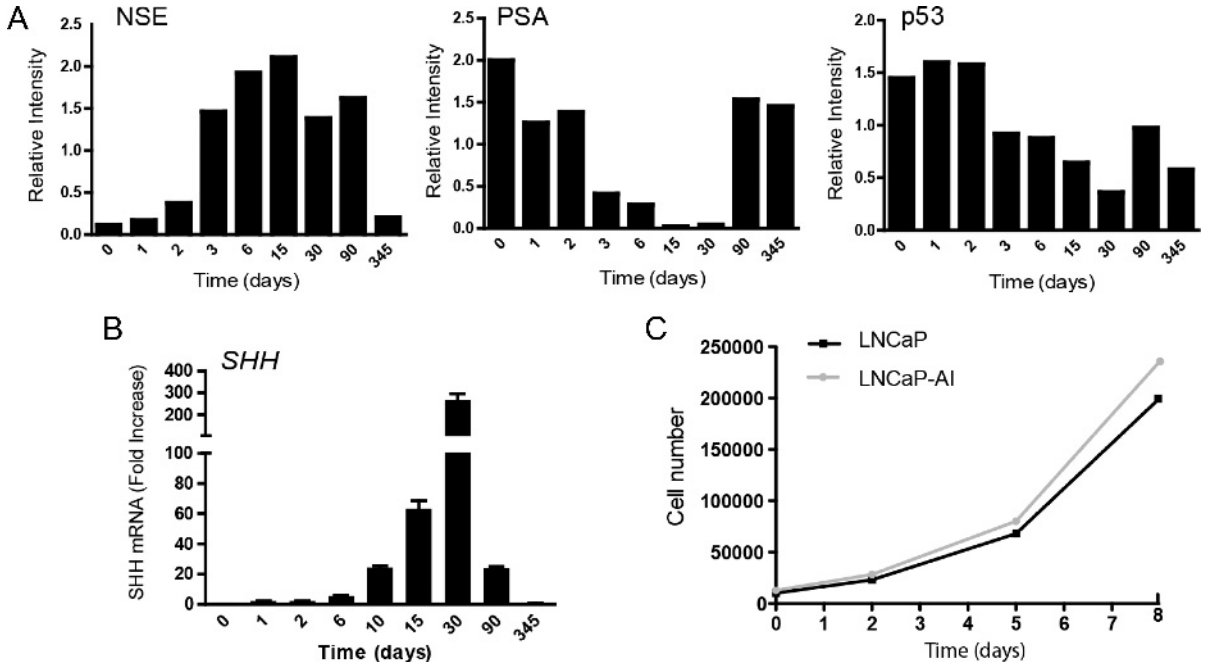

Figure W1. (A) Estimation of relative protein expression from Western blots. Densitometry of the Western blot bands for NSE, PSA, and TP53 was performed using ImageJ, and ratios of target gene to β-actin were calculated. (B) Analysis for *SHH* mRNA expression in LNCAP cells cultured in androgen-free media. Bars represent means ± SEM of two independent experiments. (C) Growth rates of LNCAP and LNCaP-AI over an 8-day period in standard medium and androgen-free media, respectively.

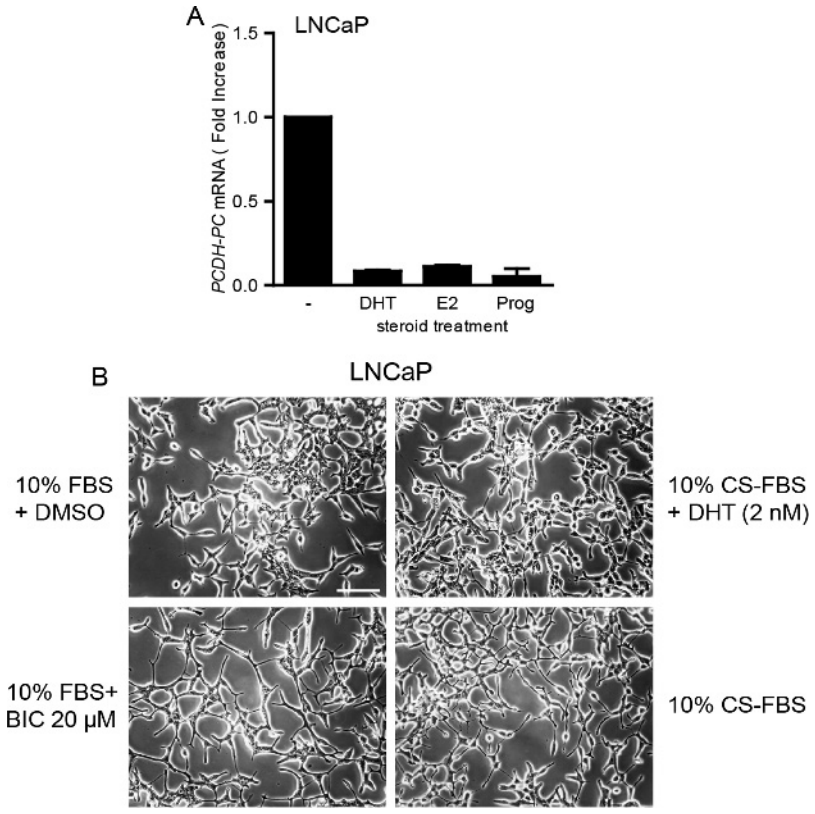

Figure W2. (A) LNCaP cells were maintained for 10 days in 10% CS-FBS media supplemented with DHT, estradiol (E_2), or progesterone at 10 nM, and PCDH-PC levels were inspected by qRT-PCR. (B) Left: Morphology of LNCaP cells grown in 10% FBS in the presence of antiandrogen bicalutamide (20 μM) or vehicle (DMSO) for 7 days. Right: Morphology of LNCaP cells in medium containing 10% CS-FBS supplemented or not with 2 nM DHT for 7 days. Scale bar, 75 μm.

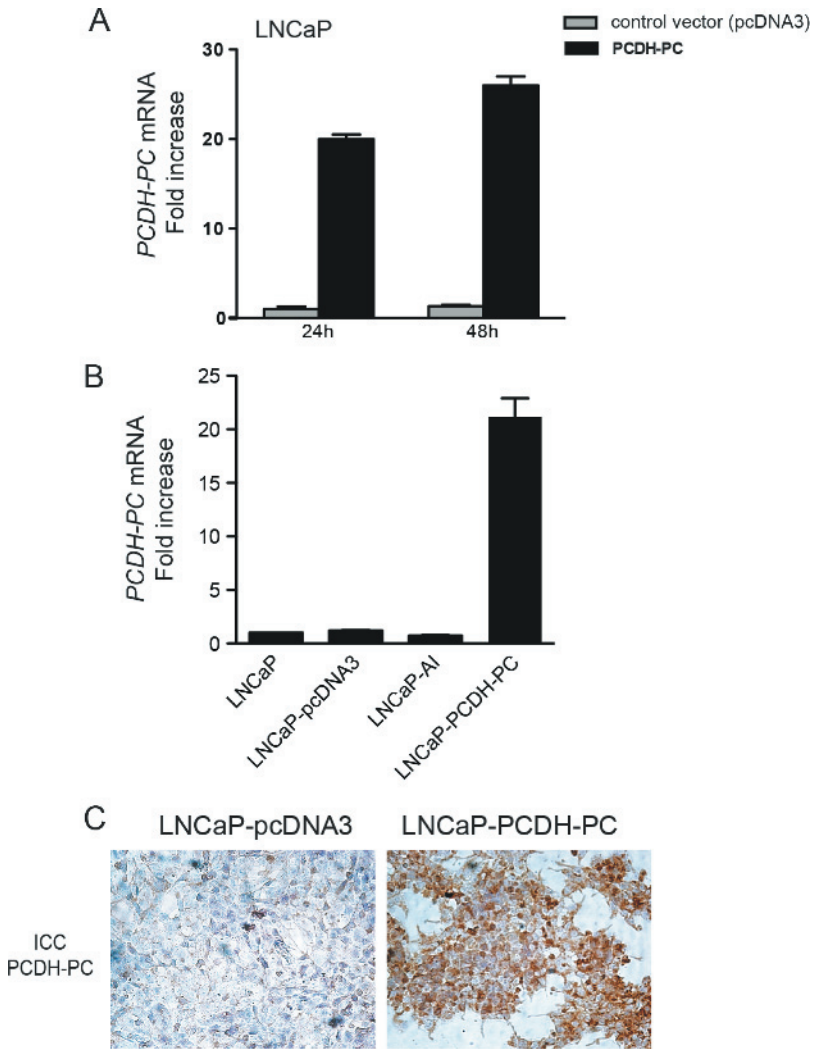

Figure W3. (A) *PCDH-PC* mRNA expression levels by qRT-PCR following transient transfection of cultures of LNCaP cells extracted at the indicated time. Data from the transfection of the empty vector were used for normalization. (B) qRT-PCR comparison of *PCDH-PC* mRNA expression levels in LNCaP, LNCaP-AI, vector, and PCDH-PC stably transfected LNCaP cells. (C) Immunocytochemistry with anti–PCDH-PC (clone HB 0337 SSA) detecting PCDH-PC in LNCaP–PCDH-PC cells but not in LNCAP-pcDNA3 cells maintained in 10% FBS containing media.

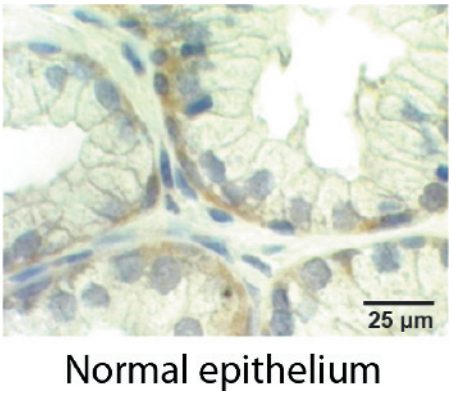

Figure W4. Immunostaining of PCDH-PC in adult normal prostate glands. (A) A faint staining was sometimes detected in the basal cells of adult prostate from young subjects.

Table W3. PCDH-PC Expression and Clinicopathologic Characteristics of 222 Evaluable Patients Who Were Treated with Radical Prostatectomy.

	PCDH-PC (Score 0 or 1)	PCDH-PC (Score 2 or 3)	
No. of patients	197	25	
Age at diagnosis median, years (range)	65 (50–75)	65 (54–74)	
Diagnostic PSA median, ng/ml (range)	9.0 (1.35–99)	8.63 (4.75–84)	
Variable	*n* (%)		
Diagnostic PSA value			
0–9.9	113 (58)	15 (60)	$P > .05$
10–20	57 (29)	6 (24)	
≥20	26 (13)	4 (16)	
Gleason score			
<7	110 (56)	11 (44)	$P > .05$
=7	49 (25)	5 (22)	
>7	37 (19)	9 (36)	
Tumor stage			
pT2	126 (64)	15 (60)	$P > .05$
pT3	61 (31)	8 (32)	
pT4	9 (5)	2 (8)	
Biologic recurrence			
No	142 (74)	19 (76)	$P > .05$
Yes	51 (26)	6 (24)	
Surgical margins			
Negative	156 (81)	18 (72)	$P > .05$
Positive	37 (19)	7 (28)	
Seminal vesicle (SV) status			
SV free	161 (83)	21 (84)	$P > .05$
SV invaded	32 (17)	4 (16)	
Positive lymph node	10 (5)	2 (8)	$P > .05$

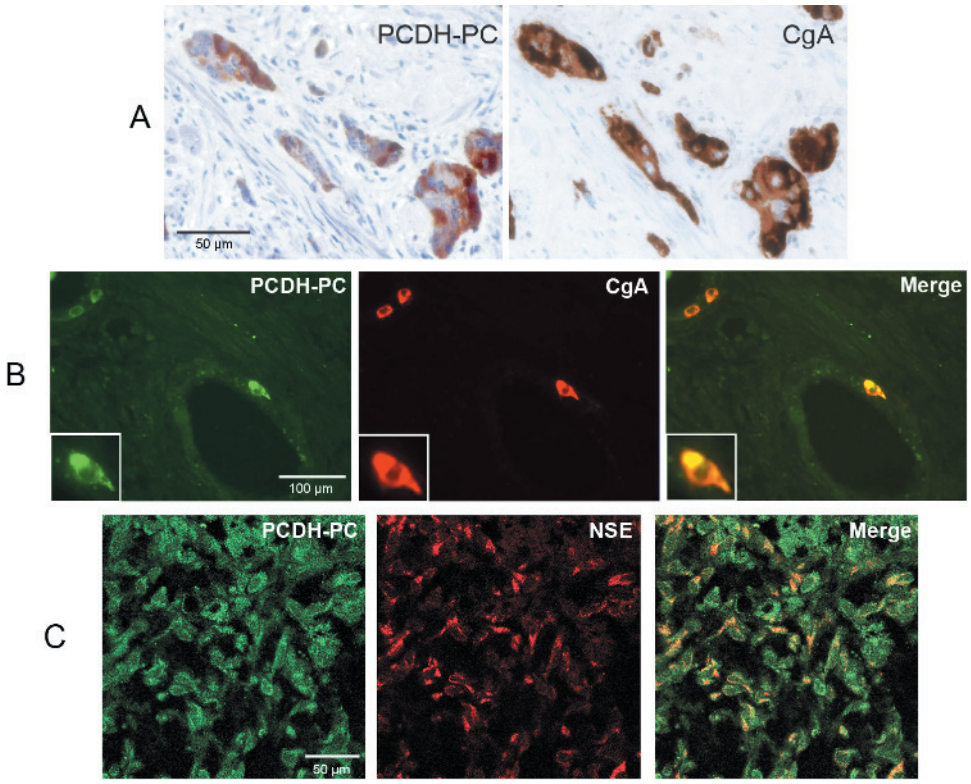

Figure W5. (A) Another case of prostatic adenocarcinoma following 6 months of ADT (LH-RH agonist therapy). All the tumor cells display NE differentiation as evidenced by intense chromogranin A cytoplasmic immunostaining and coexpress PCDH-PC with a moderate to intense cytoplasmic immunostaining. (B) Detection of CgA (in red) and PCDH-PC (in green) expression by dual immunofluorescence in a benign gland. Coexpression (in yellow) is detected in a lonely cell present within the benign epithelia of an atrophic gland. (C) PCDH-PC expression coinciding with NSE expression in PCa cells of a CRPC.

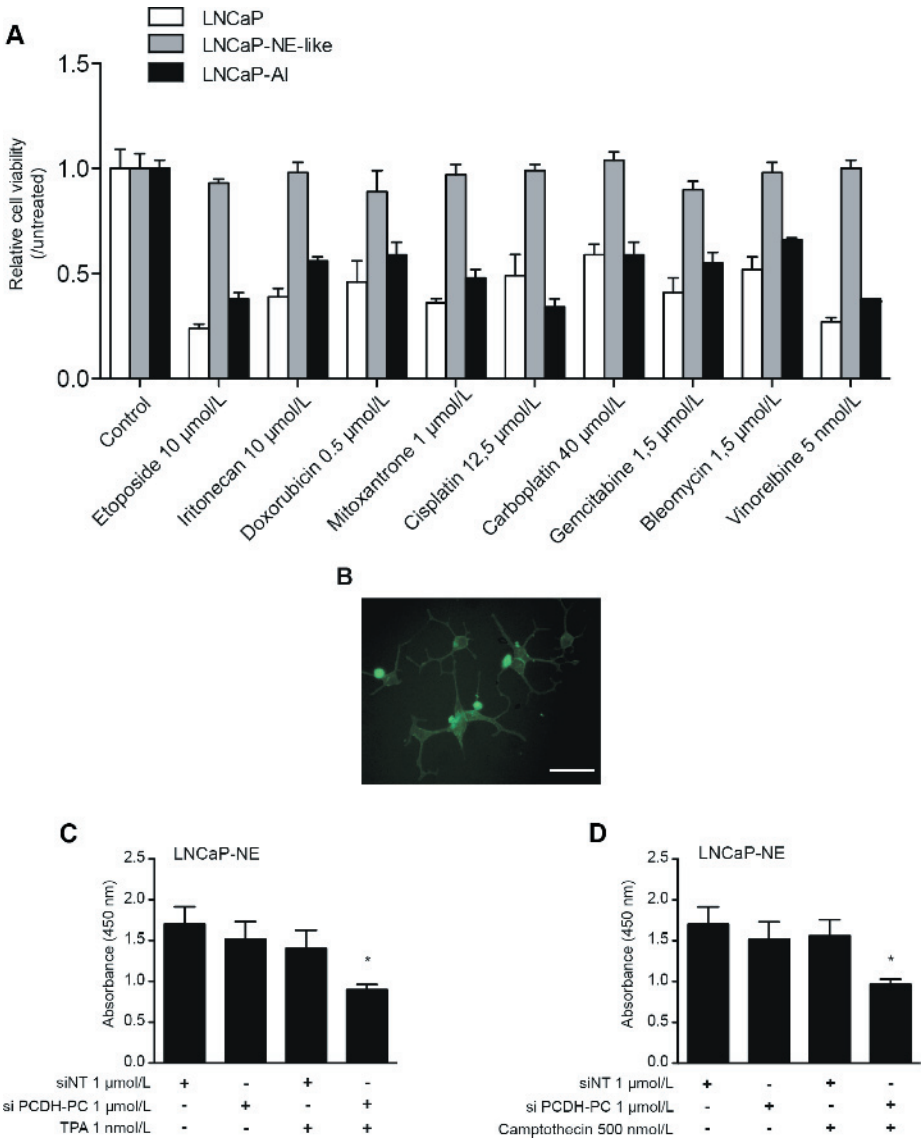

Figure W6. Acquired NE phenotype correlates with chemoresistance in LNCaP cells. (A) MTT viability assay of LNCaP (white bars), LNCaP–NE-like (gray bars), and LNCaP-AI (black bars) cells at 96 hours after treatment with different agents at the indicated doses. (B) Immunofluorescence staining of LNCaP–NE-like cells treated with Accell Green Non-Targeting siRNAs shows effective uptake of the siRNAs by the cells. (C) WST-1 cell viability assay using siRNAs treated with LNCaP–NE-like cells alone or subsequently treated with TPA for 96 hours. (D) As in C except replacing TPA by camptothecin at the indicated dose.